A functional triangle relationship of topoisomerase IIβ, BARD1, and ERK2 in immediate early gene transcription

Authors:

Heeyoun Bunch[1,2]*, Reiko Nakagawa[3], Jaehyeon Jeong[1], Anh Cong[4], Jaeyeon Jang[5], Inuk Jung[5], Keunsoo Kang[6], and Matthew J. Schellenberg[4]

Affiliations:

[1]Department of Applied Biosciences, Kyungpook National University, Daegu 41566, Republic of Korea

[2]School of Applied Biosciences, College of Agriculture & Life Sciences, Kyungpook National University, Daegu 41566, Republic of Korea

[3]RIKEN BDR Laboratory for Phyloinformatics, Hyogo 650-0047, Japan

[4]Department of Biochemistry and Molecular Biology, Mayo Clinic, Rochester, MN 55905, USA

[5]School of Computer Science and Engineering, Kyungpook National University, Daegu 41566, Republic of Korea

[6]Department of Microbiology, College of Bio-convergence, Dankook University, Cheonan 31116, Republic of Korea

*Correspondence to HB at heeyounbunch@gmail.com

ABSTRACT

Immediate early genes (IEGs) encode master transcription factors, including *EGR1*, *FOS*, *JUN*, and *MYC* genes that drive robust transcription in the G1 phase of cell cycle. Our previous studies indicate that topoisomerase IIβ (TOP2B) critically regulates IEG transcription and that the activities of TOP2B are dynamically controlled through post-translational modifications by BRCA1-BARD1 and ERKs. Here, we show that two E2 enzymes, UBCH5b and UBC13/MMS2, differentiate the effects and functions of TOP2B ubiquitination by BRCA1-BARD1. Comprehensive transcriptomics, proteomics, and biochemical and molecular cellular analyses revealed a close relationship between BARD1 and key mitogen-activated protein kinase pathway genes and identified activated ERK2 as a novel kinase that phosphorylates BARD1 at S391, a previously reported mitotic phosphorylation site, whose

genetic mutation has been linked to tumorigenesis. Mechanistically, the catalytic activity of ERK2 stimulates TOP2B ubiquitination mediated by BRCA1-BARD1 in complex with UBCH5b and UBC13/MMS2, which controls the binding and function of TOP2B and BARD1 for transcriptional activation at representative IEGs. Taken together, our data propose that there is a functional regulatory circuit involving TOP2B, BARD1, and ERK2, three key transcriptional activators for IEG transcription, in which the gene association and catalytic activity of TOP2B are regulated through E2-differentiated ubiquitination by BRCA1-BARD1 and the phosphorylation of BARD1 by ERK2 for productive transcription.

Keywords: Transcriptional regulation; topoisomerase IIβ; BARD1, ERK2; immediate early genes; RNA polymerase II transcription; gene regulation

INTRODUCTION

Metazoan transcription of messenger and most non-coding RNAs (mRNAs and ncRNAs) is carried out by a sole RNA polymerizing enzyme, RNA polymerase II (Pol II), and numerous transcription factors that act across the stages of transcriptional initiation, early elongation featuring promoter-proximal pausing/pause release, productive elongation, and termination[1-4]. These transcription factors modulate Pol II association/dissociation, polymerization and post-disengagement RNA cleavage, pausing and forward-movement, and catalytic rate[5-8]. Transcription factors and Pol II form complex, interactive and dynamically evolving networks, enabling reciprocal gene regulation in response to internal and external stimuli and cellular needs. Accumulating evidence suggests that categorizing transcriptional activators or repressors is context-dependent rather than absolute, as many transcriptional factors have biphasic functions, even in a single gene, depending on protein modifications or binding partners[9-12]. Post-translational modifications (PTMs), covalently and reversibly bonding functional inorganic or organic compounds to protein factors, are considered major molecular switches to divert functions. More than 200 distinctive PTMs have been reported, with phosphorylation and ubiquitination among the most prominent ones[13].

Protein phosphorylation is mediated by protein kinases that transfer γ-phosphates from ATP to their substrate proteins. Phosphorylation often functions as a molecular switch to turn on and off enzymatic

activities, regulates inter- and intra-molecular interactions, and determines subcellular localization and protein stability[14-16]. Ubiquitin is a small regulatory peptide (8.6 KDa), abundant and ubiquitously present in eukaryotes. Ubiquitination of a substrate protein is mediated by sequential reactions of three enzymes: an E1 ubiquitin-activating enzyme, an E2 ubiquitin-conjugating enzyme, and an E3 ubiquitin ligase[17]. There are eight E1 enzymes, approximately 40 E2 enzymes, and over 600 E3 enzymes in humans[18]. Ubiquitination has mostly been studied for proteasome-mediated proteolysis, in which K48-linked poly-ubiquitination tags misfolded, aged, or targeted proteins for degradation[19]. Short-chained ubiquitination or K63-linked polyubiquitination has been reported to regulate transcription, DNA repair, molecular interaction, translocation, and protein activity[19,20]. Recently, one study indicated the presence of non-canonical ubiquitinations by E2s, conjugating ubiquitin to serine/threonine, instead of lysine, of target proteins, without requiring E1 and E3 enzymes[21]. Together with phosphorylation, protein ubiquitination is a crucial molecular event to maintain and perform cellular processes.

BRCA1 and BARD1 proteins form a heterodimeric complex that functions as a key DNA repair factor in homologous recombination and non-canonical non-homologous end joining as well as an E3 ubiquitin ligase[22-25]. Double-stranded DNA breakage (DSB) induces DNA damage response (DDR) signaling, which activates PI3K-like kinases, ataxia telangiectasia mutated (ATM), DNA-dependent protein kinase (DNA-PK), and ataxia telangiectasia and Rad3-related (ATR)[26-28]. These kinases phosphorylate various DNA repair, cell cycle, and transcription factors, including BRCA1, TRIM28, p53, Chk1/2, γH2AX, and WRN[10,26,27,29-32]. BRCA1-BARD1 facilitates DNA resection of the broken DNA end for homologous-recombination[23]. Known ubiquitination substrates of the BRCA1-BARD1 include H2A, PCNA, NF2, estrogen receptor α, and TOP2B[22,29,33-35]. Importantly, BRCA1-BARD1 is a transcriptional activator of a subset of genes including NF-κB-responsive genes and IEGs[29,36-39]. Our previous study showed that BRCA1-BARD1 ubiquitinates TOP2B and that BARD1 interacts with TOP2B with high affinity[29]. Additionally, either BRCA1 or BARD1 knockdown (KD) destabilizes TOP2B[29]. Ubiquitinated TOP2B has a stronger affinity for the DNA fragments encompassing the *EGR1* transcription start site (TSS) in comparison with ubiquitin-stripped TOP2B, which suggests the role of BRCA1-BARD1 in the regulation of TOP2B genome association[1,29]. Supporting this finding, BRCA1 and TOP2B are co-localized genome-wide, suggesting their collaboration for gene regulation[1,29].

In IEG transcription, the cellular proliferating signal is received from the membrane receptor bound by a stimulating extracellular ligand to target genes in the nucleus through signal transduction, the well-established mitogen-activated protein kinase (MAPK) pathway[40]. A series of phosphorylation-based kinase activation cascades promote the phosphorylation/activation of ERK1 (MAPK3) and ERK2 (MAPK1) and their translocation from the cytoplasm to the nucleus[40]. Then, activated ERK2 phosphorylates and activates ELK1, a potent DNA binding transcription factor, to stimulate transcription of its target genes (e.g. *EGR1*)[14,40]. Notably, IEGs are representative examples of stress-inducible genes, where Pol II is paused in the TSSs before the reception of the activating signal[30,41-43]. Interestingly, transcriptional burst and Pol II pause release in IEGs are accompanied by and require TOP2B-mediated DDR signaling, featuring the phosphorylation and activation of ATM, DNA-PK/KU70/KU80, ATR, TRIM28, γH2AX, and BRCA1-BARD1[29,30,43,44]. It is still unclear what turns on TOP2B to mediate DNA breakage and yet, the cryo-EM structure of the etoposide-poisoned TOP2B-*EGR1* TSS complex has revealed dramatic DNA bending around a DSB, altering local DNA topology and presumably relieving DNA torsion or regulating DNA winding/helicity[14]. Consistent with this conjecture, transcriptional activation alters DNA supercoiling profiles, and DNA positive or negative supercoiling reportedly activates or represses transcription[11,45-51]. Furthermore, TOP2B knockout (KO) renders the genome to be more negatively supercoiled, underwound, and less accessible, thus deregulating transcription-mediated genomic topological changes[1,11].

Recent studies by ours and others have reported distinctive functions exerted by ERK1 and ERK2 despite about 85% identical protein primary sequences with less conserved N- and C-terminal domains (NTD and CTD)[14,52-55]. Biochemical analyses demonstrated that both ERK1 and ERK2 phosphorylate the CTD of TOP2B in mutual as well as different residues[14]. ERK1 stimulates TOP2B catalysis of both positive and negative supercoiling[14]. Interestingly, ERK2 retards TOP2B catalysis of transcriptionally favorable negative supercoiling, whereas it enhances TOP2B resolution of positive supercoiling[14]. In representative IEGs, ERK2 functions as a transcriptional activator, while ERK1 acts as a transcriptional repressor[14]. These findings are well-aligned with the reportedly distinctive roles of ERK1 and ERK2, in which only ERK2 is pro-proliferative[52-54].

In this study, we screened a total of 11 human E2 enzymes and identified E2 enzymes, UBCH5b and UBC13/MMS2 to collaborate with BRCA1-BARD1 to ubiquitinates TOP2B, yet in substantially distinct fashions. Interestingly, depleting UBCH5b or UBC13 also displays different effects on TOP2B. UBCH5b KO increases cellular TOP2B level, while reducing genome-associated TOP2B, which suggests its role in TOP2B-genome interaction and TOP2B destabilization. UBC13 KO markedly decreases TOP2B catalytic activities, as well as both cellular and chromosome-bound TOP2B protein levels. KD of either E2 enzymes or BARD1 represses IEG transcription. We found that BARD1 determines protein stability of TOP2B, UBCH5b, and UBC13 and the transcriptional output of a number of genes. Importantly, single allele deletion of BARD1 paradoxically increases key factors in MAPK pathway, including *RAF1*, *JNK*s, and *ERK*s. Mechanistically, our biochemical and mutational analyses revealed that BARD1 is phosphorylated at residue S391 by constitutively active ERK2 (ERK2m), and that ERK2 KD or catalytic inhibition results in abnormal increases of TOP2B and BARD1 occupancies and transcriptional suppression at representative IEGs. ERK2m enhances TOP2B ubiquitination by BRCA1-BARD1 with UBCH5 or UBC13/MMS2, suggesting that catalytically-active ERK2 phosphorylates BARD1 at S391 and promotes BRCA1-BARD1-mediated TOP2B ubiquitination to regulate TOP2B activity (UBC13/MMS2) and stability (UBCH5b) for transcriptional activation in IEGs.

RESULTS

BRCA1-BARD1 assembles with the E2 enzymes, UBCH5b or UBC13/MMS2, to ubiquitinate TOP2B

To identify the E2 enzymes that collaborate with the BRCA1-BARD1 complex to ubiquitinate TOP2B, 11 human E2 enzymes were screened by the *in vitro* ubiquitination and immunoblotting assays[29]. The degrees of TOP2B ubiquitination were quantified, compared with the control TOP2B from the reaction lacking an E2 enzyme. The data indicated that UBCH5b and UBC13/MMS2 are the E2 enzymes for BRCA1-BARD1 to ubiquitinate TOP2B (**Fig. 1A** and **Supplementary Figure 1A**). Next, we sought to identify the residues in TOP2B that were ubiquitinated by BRCA1-BARD1 with UBCH5b or UBC13/MMS2. TOP2B was gel-sliced after *in vitro* ubiquitination assays containing either E2 enzyme and was subjected to mass spectrometry, along with the control proteins, TOP2B, BRCA1, and BARD1 that were utilized for the *in vitro* ubiquitination assays (**Fig. 1B**). Mass spectrometry data

revealed strikingly distinct ubiquitination patterns, in particular for TOP2B, depending on the interacting E2 enzymes (**Fig. 1C, Supplementary Figure 1B,** and **Supplementary Data 1**). The ubiquitination sites on TOP2B, BARD1, and BRCA1 were marked on the primary structures (**Figs. 1C,D**). UBCH5b mediated ubiquitination of 35 residues throughout the ATPase, DNA binding & catalytic, and C-terminal domains of TOP2B. In contrast, UBC13/MMS2 in association with BRCA1-BARD1 ubiquitinated 5 residues, including K510, K744, and K979, only in DNA binding & catalytic domain (**Fig. 1C** and **Supplementary Figure 1A**). Additionally, the unique and common 66 and 36 ubiquitinated residues in BRCA1 and BARD1 were identified and mapped on the proteins (**Fig. 1D, Supplementary Figure 1C,** and **Supplementary Data 2, 3**). These data suggest that both UBCH5b and UBC13/MMS2 induce BRCA1-BARD1 to be auto-ubiquitinated at mutual and distinctive sites and that UBCH5b dictates BRCA1-BARD1 to ubiquitinate its substrate TOP2B in a more sporadic and extensive manner, while UBC13/MMS2 mediates BRCA1-BARD1 to ubiquitinate TOP2B at fewer, more specific sites in the DNA binding & catalytic domain.

BARD1, UBCH5b, or UBC13 knockdown deregulates TOP2B and represses IEG transcription

To understand the function of TOP2B ubiquitination by the two E2-E3 entities, UBCH5b-BRCA1-BARD1 and UBC13/MMS2-BRCA1-BARD1, each of BARD1, UBCH5b, and UBC13 was depleted from HEK193 cells using small interfering RNA (siRNA) species and the gene KD was validated by immunoblotting (**Fig. 2A**). Notably, we previously showed that BARD1 is important for TOP2B stability, as BARD1 KD decreases TOP2B protein levels[29]. Interestingly, UBCH5b KD significantly increased the cellular TOP2B protein level, whereas UBC13 KD mildly yet consistently decreased it (**Fig. 2B** and **Supplementary Figure 2A**). On the other hand, either UBCH5b or UBC13 KD simultaneously decreased TOP2B occupancies at the TSSs of representative IEGs, *EGR1*, *FOS*, *JUN*, and *MYC*, monitored by chromatin-immunoprecipitation-quantitative PCR (ChIP-qPCR)(**Fig. 2C** and **Supplementary Figure 2B**). Additionally, we monitored TOP2A occupancies at the IEGs in the control and KD cells because TOP2A has emerging roles in transcriptional regulation and may play mutual and distinctive roles from ones of TOP2B[1,56-58]. ChIP-qPCR results, comparing the control (scrambled siRNA, SCR) and KD cells, showed that TOP2A association with these genes was also compromised, similarly to the case of TOP2B (**Fig. 2D** and **Supplementary Figure 2C,D**), suggesting that BARD1, UBCH5b, and UBC13 might also ubiquitinate and regulate TOP2A. Despite

the interesting findings with TOP2A, we decided to carry out the experiments solely focusing on TOP2B as our main protein of interest in this study.

Genome-bound TOP2B levels were compared through the *in vivo* complex of enzymes (ICE) assay. Although UBCH5b KD significantly increased cellular TOP2B levels, it did not increase but decreased chromosome-bound TOP2B (**Figs. 3B,E** and **Supplementary Figure 2E**). Consistently with the decreased cellular TOP2B levels, UBC13 KD reduced TOP2B-chromosome association (**Fig. 3B,E** and **Supplementary Figure 2E**). Using etoposide, a small chemical inhibitor that traps TOP2 in the TOP2-DNA cleavage complex, which is otherwise a transient intermediate[14], genome-wide TOP2B catalytic activity was compared in the SCR control, UBCH5b, and UBC13 KD cells. UBC13 KD markedly reduced TOP2B catalytic activities, while only a slight reduction was observed in UBCH5b KD cells (**Fig. 3E**). These results suggested that UBCH5b KD may enhance TOP2B association with the chromosome without critically affecting TOP2B catalysis, whereas UBC13 KD may decrease TOP2B protein stability and catalysis on the chromosomes.

We assessed the effects of BARD1, UBCH5b, or UBC13 KD on IEG transcription by quantitative real-time PCR (qRT-PCR). The data showed that these factors are required for full transcription efficiency at representative IEGs (**Fig. 2F**). The mRNA expression of representative IEGs, *EGR1*, *FOS*, and *JUN*, was compared between the control and KD cells, in serum-starvation (S0) and serum-induction for 15 min (S15). The data indicated that BARD1, UBCH5b, or UBC13 KD interferes with transcription at these genes in both S0 and S15 conditions (**Fig. 2G** and **Supplementary Figure 2B,C**). Overall, our data shown in **Figs. 1** and **2** suggest the distinct patterns and roles of BRCA1-BARD1-mediated TOP2B ubiquitination, determined by UBCH5b and UBC13/MMS2. Although both E2 enzymes and BARD1 are important for TOP2B function and IEG transcription, UBCH5b-mediated TOP2B ubiquitination appears to regulate TOP2B-gene association and TOP2B protein degradation, whereas UBC13/MMS2-mediated TOP2B ubiquitination is likely to control TOP2B stability and catalytic activity.

A transcription-regulatory circuit between BARD1 and mitogen-activated protein kinase pathway

We sought to understand the regulatory mechanisms of the BRCA1-BARD1 complex-mediated TOP2B ubiquitination. To screen the genes, whose expression is directly or indirectly regulated by BARD1, CRISPR-Cas9 BARD1 KO was performed using gRNAs targeting the exon 4 (**Supplementary Data 4,5**). As previously reported, homozygous BARD1 KO was also lethal[59] in our trial, and we could obtain only a heterozygous BARD1 KO (BARD1 KO^{hz}) HEK293 cell line for this work. BARD1 KO^{hz} was confirmed by PCR, genomic sequencing (**Supplementary Data 4,5**), and immunoblotting (**Fig. 3A** and **Supplementary Figure 3A**). As described previously, the TOP2B protein level was markedly reduced along with a decreased BARD1 protein level in BARD1 KO^{hz} cells (**Fig. 3A**). TOP2A level was mildly reduced, whereas the γH2AX level was notably elevated in BARD1 KO^{hz} cells (**Fig. 3A** and **Supplementary Figure 3A**), suggesting elevated genomic instability in BARD1 lacking cells. Interestingly, we found the opposing effects of BARD1 KO on cellular UBCH5b and UBC13 protein levels. In BARD1 KO^{hz} cells, UBCH5b was increased, while the UBC13 level was diminished (molecular weight of UBCH5b and UBC13, approximately 17 KDa**; Fig. 3B**).

Total RNA-seq comparing WT and BARD1 KO^{hz} cells revealed that a larger number of genes were downregulated [Log_2 fold change (FC) < 1; $p < 0.05$; n = 1686] and a smaller number of genes were upregulated in BARD1 KO^{hz} cells [Log_2 fold change (FC) > 1; $p < 0.05$; n = 298](**Fig. 3C** and **Supplementary Data 6**). We could see the mRNA levels of representative IEGs, including *EGR1*, *MYC*, *FOS*, and *JUN*, were significantly decreased in BARD1 KO^{hz} cells, consistently with the qRT-PCR results comparing WT and BARD1 KD cells (**Figs. 2F,G,3C,D** and **Supplementary Figure 3B**). A heatmap depicting differentially expressed genes (DEGs) upon BARD1 KO^{hz} was shown in **Fig. 3E**. KEGG pathway analysis projected neuroactive ligand-receptor interaction and the MAPK pathway as the most affected pathways in BARD1 KO^{hz} cells (**Fig. 3F**). For the neuroactive ligand-receptor interaction, we note that recent studies have indicated an important, bidirectional kidney-brain axis to regulate kidney and brain functions and a few critical neuronal gene expressions in kidney[60,61]. It was particularly interesting to learn that BARD1 KO affects the MAPK pathway because it is the pathway well-known to stimulate the IEG expression. The expression of critical MAPK pathway genes[40], including *RAF1*, *NRAS*, *HRAS*, *JNK1*, *JNK2*, *ERK1*, and *ERK2*, was monitored, comparing WT and BARD1 KO^{hz} cells. Intriguingly, these key players of the MAPK pathway were mildly yet significantly upregulated in BARD1 KO^{hz} cells (**Figs. 3G,H** and **Supplementary Data 7**). It seemed paradoxical that BARD1 deletion could cause the increased expression of key genes in MAPK pathway, while

decreasing critical target genes of the MAPK pathway (**Figs. 3C,D,G,H** and **Supplementary Figure 3B**). BARD1 is a DNA binding protein (**Supplementary Figure 3C**) and stably associated with IEG promoters[29]. Based on the unexpected findings and spatial and temporal relations between BARD1 and ERKs, we hypothesized whether BARD1 could be a downstream effector regulated by these MAPK pathway proteins, to control the expression of IEGs.

Activated ERK2 phosphorylates BARD1 at S391, a pathologically important residue for IEG activation

To test the hypothesis, BARD1 protein was expressed and purified from HEK293 cells. Human ERK1 and ERK2 and well-characterized, constitutively active R84S ERK1 (ERK1m) and R67S ERK2 (ERK2m) mutants[14,62] were purified from bacteria as described in our previous work[14]. The purified proteins were subjected to the *in vitro* kinase assay using ^{32}P-radioactive ATP. We found that BARD1 was phosphorylated by ERK1m and ERK2m (**Fig. 4A**). Notably, ERK1 could be auto-phosphorylated, which was a previously unknown phenomenon, while ERK2 could not, and both unmodified ERK1 and ERK2 did not phosphorylate BARD1 (**Fig. 4A**). Next, we performed the *in vitro* kinase assay with cold ATP, and the bands corresponding to BARD1 on the SDS gel, separating the control (ERK storage buffer only), BARD1-ERK1m, and BARD1-ERK2m reactions, were analyzed by phospho-peptide enrichment mass spectrometry analyses (**Figs. 4B,C**). The mass spectrometry data indicated a residue S394 in the control BARD1 and a phosphorylation of S391 uniquely by ERK2m with high confidence (**Fig. 4D**, **Supplementary Figure 4A**, and **Supplementary Data 8–12**). Interestingly, the residue S391 has been reported as a mitotic BARD1 phosphorylation site and its mutations have been implicated in cancers[59,63]. The kinase has been unknown so far, and to our best knowledge, this is the first study that unveiled that activated ERK2 is responsible for BARD1 phosphorylation at S391 (**Figs. 4A–D**, **Supplementary Figure 4A**, and **Supplementary Data 8–12**).

We investigated the effect of ERK2-mediated BARD1 phosphorylation on IEG transcription and BARD1-gene interaction. VX-11e (VX11), a small chemical inhibitor specific to ERK2[64,65], was employed, and the occupancies of BARD1 and phosphorylated Pol II at S2 of the RPB1 subunit (S2 Pol II) were monitored in serum-starvation and -induction, S0 and S15 conditions. VX11 was supplemented to the cells at a final concentration of 100 nM for 3 h with the control dimethyl sulfoxide (DMSO) side-by-side. Strikingly, ERK2 catalytic inhibition by VX11 significantly increased the BARD1

level associated with the TSSs of *EGR1* and *FOS* (**Fig. 4F**). By contrast, upon serum-induced gene activation, S2 Pol II levels were notably decreased in the gene bodies of *EGR1* and *FOS* in the presence of VX11 (S15, **Fig. 4G**). Additionally, we depleted ERK2 using siRNA species targeting ERK2 and found that ERK2 KD increased BARD1 occupancies in the TSSs of *EGR1* and *FOS*, similarly to the results from ERK2 catalytic inhibition (**Fig. 4H** and **Supplementary Figure 4B**). As shown in our previous study[14], VX11 treatment or ERK2 KD increased TOP2B occupancies in the TSSs of *EGR1* and *FOS* genes. Together, these data suggested that ERK2-mediated phosphorylation of BARD1 is required for proper BARD1 association and function and transcriptional activation in IEGs.

BARD1 phosphorylation by activated ERK2 enhances UBCH5b- and UBC13/MMS2-mediated TOP2B ubiquitination

For mechanistic understanding of ERK2-mediated BARD1 phosphorylation in TOP2B ubiquitination by BRCA1-BARD1 with UBCH5b or UBC13/MMS, each of the BRCA1-BARD1 complex, TOP2B, and ERK2m proteins was prepared through a series of liquid chromatography procedures, as previously established (**Fig. 5A**)[14,29] and validated by immunoblotting (**Fig. 5B**). These proteins along with E1 and two E2 enzymes, UBCH5b and UBC13 were utilized for the *in vitro* ubiquitination assay. To inhibit ERK2m kinase activity, VX11 was supplemented to the designated reactions at 1 μM final concentration. E1 (approximately 120 KDa) and BRCA1-BARD1 (220 KDa and 100 KDa) as the E3 ligase were added in minimal amounts (1–50 nM) to avoid signal overlapping as their molecular weights are similar to the one of TOP2B (180 KDa). Approximately 22% of each terminated reaction was visualized by SDS-PAGE and silver-staining, validating equivalence among reactions and any visible protein degradation (**Fig. 5C**). TOP2B ubiquitination and TOP2B were monitored by immunoblotting. The results revealed enhanced TOP2B ubiquitination by BRCA1-BARD1-UBCH5b in the presence of ERK2m, with more smearing upper bands and a prominent band with a higher molecular weight (red boxes for comparison and a red asterisk for the upper band, **Fig. 5D**). BRCA1-BARD1-UBC13/MMS2 robustly ubiquitinated TOP2B, and the presence of ERK2m apparently further enhanced TOP2B ubiquitination by the complex (light blue boxes for comparison, **Fig. 5D**). VX11 overturned ERK2m-stimulated TOP2B ubiquitination, to the levels similar to the control reactions without ERK2m (yellow boxes, **Fig. 5D**), further confirming the novel function of activated ERK2 in stimulating BRCA1-BARD1 coupled with UBCH5b or UBC13/MMS2 to ubiquitinate TOP2B.

DISCUSSION

Metazoan stress-inducible gene regulation employs a systematic regulatory step downstream of the TSS, immediately before productive elongation, called Pol II pausing and pause release[15,66]. This step ensures a prompt and synchronized transcriptional burst to maximize the efficiency of gene regulation, for genes that must respond rapidly to cellular signals. We have been studying the mechanisms of Pol II pausing and pause release, using representative Pol II pausing model genes, such as *HSP70*, hypoxia-inducible genes (HIGs), and IEGs[10,11,14,29,30,67]. In particular, *HSP70*, *EGR1*, and *FOS* display well-established, prominent Pol II pausing and their expression is profoundly dependent on complex regulatory networks that convert paused Pol II into a processive enzyme. For example, the catalytic activity of TOP2B and DDR signaling are required for productive transcription in IEGs[1,14,30,41]. Inhibiting TOP2B or DNA-PK using small chemical inhibitors prevents Pol II from being released from pausing and hinders transcriptional activation in IEGs. Whether TOP2B causes DSBs as a programmed, gene regulatory custom or as a random, accidental event remains as debatable, however, it has been shown that TOP2B-mediated DSBs activate transcription in diverse sets of genes[14,30,43,68,69]. For example, etoposide, trapping TOP2B after the generation of DSB, stimulates IEG transcription, whereas ICRF193, a TOP2B catalytic inhibitor, represses it[14,30]. The sequence of events is presumably that TOP2B is modulated by a transcription factor(s) or DNA topological stresses to become catalytically active; TOP2B mediates DSB to condition DNA topology to be favorable for transcription; DSB provokes DDR signaling; DNA repair factors are activated, which should be validated in the future.

To understand the upstream factors or events that regulate TOP2B binding to genes and catalysis, we have been investigating key transcription factors implicated in Pol II pause release, including BRCA1-BARD1, DNA-PK, and ERKs[1,11,14,29,30]. Among these factors, BARD1, TOP2B, and DNA-PK are abundantly associated with TSSs of the genes harboring Pol II pausing during the transcriptionally resting state[29,30]. Previously, it was shown that BRCA1-BARD1 ubiquitinates TOP2B and contributes to increased TOP2B stability and affinity to DNA in the Pol II pausing state[29]. Transcriptional activation is coupled with DDR signaling in IEGs, provoking the activation of ATM to phosphorylate BRCA1 at S1524, γH2AX, and DNA-PK[1,29,30,41]. Furthermore, ERK2 can directly

phosphorylate TOP2B to control TOP2B catalysis of positive and negative DNA supercoiling[14]. Interestingly, ERK2 promotes TOP2B to resolve positive supercoiling and yet, delays it to relax negative DNA supercoiling[14].

The findings of this work deepen the mechanistic understanding of the dynamic interactions and regulations among these important transcriptional, DNA repair, and DNA topological factors (**Fig. 6**). First, we found that BRCA1-BARD1-mediated TOP2B ubiquitination as differential effects on TOP2B behaviors depending on the engaging E2 enzymes, UBCH5b vs UBC13/MMS2 (**Figs. 1A–D,2B,E,5D** and **Supplementary Figures 1A–D,2A**). UBCH5b is a universal E2 known to mediate K48-linked polyubiquitination, for promoting protein destabilization and DNA repair [70,71,72], whereas UBC13 is a more specialized E2 to synthesize K63-linked polyubiquitination for signal transduction and DNA repair[73,74]. UBCH5b KD elevated cellular TOP2B protein levels without affecting its genome activities (**Figs. 2B,E** and **Supplementary Figure 2A**), while compromising IEG transcription (**Figs. 2F,G**), which suggests that UBCH5b-mediated TOP2B dissociation/destabilization might be important for proper IEG transcriptional activation. UBC13 KD decreased both cellular protein levels and the genome-wide activities of TOP2B as well as IEG transcription (**Figs. 2B,E,F,G** and **Supplementary Figures 2A**), suggesting that UBC13-mediated TOP2B ubiquitination could be required for TOP2B stability and catalysis in IEG transcription. Second, our work identified a bidirectional relationship between the MAPK pathway and BARD1 and discovered activated ERK2 as a novel kinase that phosphorylates BARD1 at S391 (**Figs. 3E–H,4A–E**). Recent studies have emphasized the functional crosstalk between DDR and MAPK pathway for the determination of cell fate and its abnormality in cancers[75,76]. It is notable that BARD1 KD markedly increases cellular γH2AX levels (**Fig. 3A** and **Supplementary Figure 3A**), implying the accumulation of genomic instability, which may contribute to the activation of key players in the MAPK pathway. Additionally, our data suggest an important role of BARD1 and BARD1-mediated ubiquitination of its substrates (e.g., TOP2B) for IEG transcription in response to a MAPK pathway activation, because IEG expression is diminished without BARD1, despite significantly increased levels of key MAPK pathway genes (**Figs. 2A,F,G,3A,C,D** and **Supplementary Figure 3B**). Third, activated ERK2-mediated BARD1 phosphorylation stimulates TOP2B ubiquitination by both E2–E3 complexes, UBCH5b-BRCA1-BARD1 and UBC13/MMS2-BRCA1-BARD1 (**Fig. 5D**). Inhibiting such phosphorylation results in abnormal increases/retentions of BARD1 and TOP2B and transcriptional repression in IEGs (**Figs. 4F–I**). We suggest that the

stimulation of BARD1-mediated TOP2B ubiquitination by activated ERK2, in conjunction with UBCH5b and UBC13/MMS2, is important for proper TOP2B dissociation/mobilization and catalysis and thus for transcriptional activation.

Recent studies by others and our own have shown distinctive Pol II pausing regulatory mechanisms in HIGs in comparison to what has been understood in IEGs[1,11,77]. The most critical difference is that DDR seems rarely involved in Pol II pause release in HIGs, although similar DNA repair factors play key roles in Pol II pausing and pause release, including DNA-PK, TRIM28, and TOP2B in both IEGs and HIGs[30,77]. These gene-specific differential mechanisms may be explained by genomic context-dependent DNA topological signatures and requirements[1,11]. For instance, TOP2B inhibition by small chemicals has different effects on IEGs and HIGs[1,11,14,30]. In HIGs, TOP2B is phosphorylated at T1403 by DNA-PK in the state of Pol II pausing, in which the activity of TOP2B plays an important role in suppressing HIG transcription in the resting state, under normoxia[11]. In contrast, in IEGs, TOP2B catalysis is activated upon transcriptional activation[14,29,30,43]. For example, activated ERK2 phosphorylates and catalytically activates BARD1 and TOP2B, as shown previously and in this study (**Figs. 4F–I,5D** and **Supplementary Figure 4A**)[14]. The exact role of DNA-PK phosphorylation/activation in transcriptional activation of subsets of genes such as HIGs, IEGs, *HSP70*, and androgen- and estrogen-receptor genes remains to be uncovered[10,11,30,68,69,77,78]. In particular, BRCA1-BARD1 and DNA-PK reportedly compete for distinctive DSB repair pathways to be engaged with the DSB sites[79,80]. Is this the reason why these factors co-occupy IEGs, or are there other unknown molecular dynamics involving them? Moreover, it will be interesting to understand what mediates and regulates specific E2 enzymes to interact with BRCA1-BARD1 during Pol II pausing and pause release in IEG transcription. These are some of the critical questions awaiting future investigations.

References

1. Bunch, H. DNA topological regulation in RNA polymerase II transcription. *Cell Mol Biol Lett* **31**(2026).
2. Ebmeier, C.C. & Taatjes, D.J. Activator-Mediator binding regulates Mediator-cofactor interactions. *Proc Natl Acad Sci U S A* **107**, 11283-8 (2010).
3. Lysakovskaia, K., Devadas, A., Schwalb, B., Lidschreiber, M. & Cramer, P. Promoter-proximal RNA polymerase II termination regulates transcription during human cell type transition. *Nat Struct Mol Biol* **32**, 995-1005 (2025).

4. Bunch, H. Gene regulation of mammalian long non-coding RNA. *Mol Genet Genomics* **293**, 1-15 (2018).
5. Sheridan, R.M., Fong, N., D'Alessandro, A. & Bentley, D.L. Widespread Backtracking by RNA Pol II Is a Major Effector of Gene Activation, 5' Pause Release, Termination, and Transcription Elongation Rate. *Mol Cell* **73**, 107-118 e4 (2019).
6. Lee, C. et al. NELF and GAGA factor are linked to promoter-proximal pausing at many genes in Drosophila. *Mol Cell Biol* **28**, 3290-300 (2008).
7. Li, J. et al. Kinetic Competition between Elongation Rate and Binding of NELF Controls Promoter-Proximal Pausing. *Mol Cell* **50**, 711-22 (2013).
8. Lis, J.T., Mason, P., Peng, J., Price, D.H. & Werner, J. P-TEFb kinase recruitment and function at heat shock loci. *Genes Dev* **14**, 792-803 (2000).
9. Ping, Y.H. & Rana, T.M. DSIF and NELF interact with RNA polymerase II elongation complex and HIV-1 Tat stimulates P-TEFb-mediated phosphorylation of RNA polymerase II and DSIF during transcription elongation. *J Biol Chem* **276**, 12951-8 (2001).
10. Bunch, H. et al. TRIM28 regulates RNA polymerase II promoter-proximal pausing and pause release. *Nat Struct Mol Biol* (2014).
11. Bunch, H. et al. DNA topological regulation by topoisomerase IIβ-DNA-PK interaction is important for controlled hypoxia-inducible gene expression. *bioRxiv*, 2025.01.06.631366 (2025).
12. Zhang, J. et al. Dependency of NELF-E-SLUG-KAT2B epigenetic axis in breast cancer carcinogenesis. *Nat Commun* **14**, 2439 (2023).
13. Vellosillo, P. & Minguez, P. A global map of associations between types of protein posttranslational modifications and human genetic diseases. *iScience* **24**, 102917 (2021).
14. Bunch, H. et al. ERK2-topoisomerase II regulatory axis is important for gene activation in immediate early genes. *Nat Commun* **14**, 8341 (2023).
15. Bunch, H. HSF1 in RNA Polymerase II Promoter-Proximal Pausing and HSP70 Transcription. in *Heat Shock Proteins in Inflammatory Diseases* (eds. Asea, A.A.A. & Kaur, P.) 489-508 (Springer International Publishing, Cham, 2021).
16. Potel, C.M. et al. Impact of phosphorylation on thermal stability of proteins. *Nat Methods* **18**, 757-759 (2021).
17. Damgaard, R.B. The ubiquitin system: from cell signalling to disease biology and new therapeutic opportunities. *Cell Death Differ* **28**, 423-426 (2021).
18. Stewart, M.D., Ritterhoff, T., Klevit, R.E. & Brzovic, P.S. E2 enzymes: more than just middle men. *Cell Res* **26**, 423-40 (2016).
19. Rahman, S. & Wolberger, C. Breaking the K48-chain: linking ubiquitin beyond protein degradation. *Nat Struct Mol Biol* **31**, 216-218 (2024).
20. Dosa, A. & Csizmadia, T. The role of K63-linked polyubiquitin in several types of autophagy. *Biol Futur* **73**, 137-148 (2022).
21. Abdul Rehman, S.A. et al. Discovery and characterization of noncanonical E2-conjugating enzymes. *Sci Adv* **10**, eadh0123 (2024).
22. Salas-Lloret, D. et al. BRCA1/BARD1 ubiquitinates PCNA in unperturbed conditions to promote continuous DNA synthesis. *Nat Commun* **15**, 4292 (2024).
23. Ceppi, I. et al. Mechanism of BRCA1-BARD1 function in DNA end resection and DNA protection. *Nature* **634**, 492-500 (2024).
24. Salunkhe, S. et al. Promotion of DNA end resection by BRCA1-BARD1 in homologous recombination. *Nature* **634**, 482-491 (2024).

25. Jiang, G. et al. BRCA1-Ku80 protein interaction enhances end-joining fidelity of chromosomal double-strand breaks in the G1 phase of the cell cycle. *J Biol Chem* **288**, 8966-76 (2013).
26. Gatei, M. et al. Role for ATM in DNA damage-induced phosphorylation of BRCA1. *Cancer Res* **60**, 3299-304 (2000).
27. Chen, B.P. et al. Ataxia telangiectasia mutated (ATM) is essential for DNA-PKcs phosphorylations at the Thr-2609 cluster upon DNA double strand break. *J Biol Chem* **282**, 6582-7 (2007).
28. Kemp, M.G. DNA damage-induced ATM- and Rad-3-related (ATR) kinase activation in non-replicating cells is regulated by the XPB subunit of transcription factor IIH (TFIIH). *J Biol Chem* **292**, 12424-12435 (2017).
29. Bunch, H. et al. BRCA1-BARD1 regulates transcription through modulating topoisomerase IIbeta. *Open Biol* **11**, 210221 (2021).
30. Bunch, H. et al. Transcriptional elongation requires DNA break-induced signalling. *Nat Commun* **6**, 10191 (2015).
31. Pichierri, P., Rosselli, F. & Franchitto, A. Werner's syndrome protein is phosphorylated in an ATR/ATM-dependent manner following replication arrest and DNA damage induced during the S phase of the cell cycle. *Oncogene* **22**, 1491-500 (2003).
32. Stokes, M.P. et al. Profiling of UV-induced ATM/ATR signaling pathways. *Proc Natl Acad Sci U S A* **104**, 19855-60 (2007).
33. Kalb, R., Mallery, D.L., Larkin, C., Huang, J.T. & Hiom, K. BRCA1 is a histone-H2A-specific ubiquitin ligase. *Cell Rep* **8**, 999-1005 (2014).
34. Verma, S. et al. BRCA1/BARD1-dependent ubiquitination of NF2 regulates Hippo-YAP1 signaling. *Proc Natl Acad Sci U S A* **116**, 7363-7370 (2019).
35. Ma, Y. et al. BRCA1 regulates acetylation and ubiquitination of estrogen receptor-alpha. *Mol Endocrinol* **24**, 76-90 (2010).
36. Benezra, M. et al. BRCA1 augments transcription by the NF-kappaB transcription factor by binding to the Rel domain of the p65/RelA subunit. *J Biol Chem* **278**, 26333-41 (2003).
37. Welcsh, P.L. et al. BRCA1 transcriptionally regulates genes involved in breast tumorigenesis. *Proc Natl Acad Sci U S A* **99**, 7560-5 (2002).
38. Mullan, P.B., Quinn, J.E. & Harkin, D.P. The role of BRCA1 in transcriptional regulation and cell cycle control. *Oncogene* **25**, 5854-63 (2006).
39. Gardini, A., Baillat, D., Cesaroni, M. & Shiekhattar, R. Genome-wide analysis reveals a role for BRCA1 and PALB2 in transcriptional co-activation. *EMBO J* **33**, 890-905 (2014).
40. Zhang, W. & Liu, H.T. MAPK signal pathways in the regulation of cell proliferation in mammalian cells. *Cell Res* **12**, 9-18 (2002).
41. Bunch, H. Role of genome guardian proteins in transcriptional elongation. *FEBS Lett* **590**, 1064-75 (2016).
42. Ohe, S. et al. ERK-mediated NELF-A phosphorylation promotes transcription elongation of immediate-early genes by releasing promoter-proximal pausing of RNA polymerase II. *Nat Commun* **13**, 7476 (2022).
43. Madabhushi, R. et al. Activity-Induced DNA Breaks Govern the Expression of Neuronal Early-Response Genes. *Cell* **161**, 1592-605 (2015).
44. Bunch, H. Studying RNA Polymerase II Promoter-Proximal Pausing by In Vitro Immobilized Template and Transcription Assays. *Methods Mol Biol* **2693**, 13-24 (2023).

45. Stolz, R. et al. Interplay between DNA sequence and negative superhelicity drives R-loop structures. *Proc Natl Acad Sci U S A* **116**, 6260-6269 (2019).
46. Fogg, J.M., Judge, A.K., Stricker, E., Chan, H.L. & Zechiedrich, L. Supercoiling and looping promote DNA base accessibility and coordination among distant sites. *Nat Commun* **12**, 5683 (2021).
47. Guo, M.S., Kawamura, R., Littlehale, M.L., Marko, J.F. & Laub, M.T. High-resolution, genome-wide mapping of positive supercoiling in chromosomes. *Elife* **10**(2021).
48. Hwang, J. et al. DNA supercoiling-mediated G4/R-loop formation tunes transcription by controlling the access of RNA polymerase. *Nat Commun* **16**, 3363 (2025).
49. Patel, H.P. et al. DNA supercoiling restricts the transcriptional bursting of neighboring eukaryotic genes. *Mol Cell* **83**, 1573-1587 e8 (2023).
50. Mizutani, M., Ohta, T., Watanabe, H., Handa, H. & Hirose, S. Negative supercoiling of DNA facilitates an interaction between transcription factor IID and the fibroin gene promoter. *Proc Natl Acad Sci U S A* **88**, 718-22 (1991).
51. Leng, F. & McMacken, R. Potent stimulation of transcription-coupled DNA supercoiling by sequence-specific DNA-binding proteins. *Proc Natl Acad Sci U S A* **99**, 9139-44 (2002).
52. Woodson, E.N. & Kedes, D.H. Distinct roles for extracellular signal-regulated kinase 1 (ERK1) and ERK2 in the structure and production of a primate gammaherpesvirus. *J Virol* **86**, 9721-36 (2012).
53. Bosso, G. et al. Differential contribution for ERK1 and ERK2 kinases in BRAF(V600E)-triggered phenotypes in adult mouse models. *Cell Death Differ* **31**, 804-819 (2024).
54. Gagliardi, M. et al. Differential functions of ERK1 and ERK2 in lung metastasis processes in triple-negative breast cancer. *Sci Rep* **10**, 8537 (2020).
55. Ju, S. et al. Novel DNA endonuclease activity of human ERK1 protein. *bioRxiv*, 2025.03.03.641133 (2025).
56. Pommier, Y., Sun, Y., Huang, S.N. & Nitiss, J.L. Roles of eukaryotic topoisomerases in transcription, replication and genomic stability. *Nat Rev Mol Cell Biol* **17**, 703-721 (2016).
57. Das, S.K. et al. MYC assembles and stimulates topoisomerases 1 and 2 in a "topoisome". *Mol Cell* **82**, 140-158 e12 (2022).
58. Herrero-Ruiz, A. et al. Topoisomerase IIalpha represses transcription by enforcing promoter-proximal pausing. *Cell Rep* **35**, 108977 (2021).
59. Choudhury, A.D. et al. Hyperphosphorylation of the BARD1 tumor suppressor in mitotic cells. *J Biol Chem* **280**, 24669-79 (2005).
60. Zuo, M. et al. The relationship between kidney health and neurodegenerative diseases. *Brain* **148**, 2616-2630 (2025).
61. Cao, W. et al. A kidney-brain neural circuit drives progressive kidney damage and heart failure. *Signal Transduct Target Ther* **8**, 184 (2023).
62. Smorodinsky-Atias, K. et al. Intrinsically active variants of Erk oncogenically transform cells and disclose unexpected autophosphorylation capability that is independent of TEY phosphorylation. *Mol Biol Cell* **27**, 1026-39 (2016).
63. Richards, S. et al. Standards and guidelines for the interpretation of sequence variants: a joint consensus recommendation of the American College of Medical Genetics and Genomics and the Association for Molecular Pathology. *Genet Med* **17**, 405-24 (2015).
64. Muthukumar, V., Vashishth, A., Maniam, S. & Ghosh, B. Molecular Frameworks for ERK1/2 Inhibition: Lessons from Synthetic and SAR Explorations. *ACS Omega* **10**, 62407-62426 (2025).

65. Pegram, L.M. et al. Activation loop dynamics are controlled by conformation-selective inhibitors of ERK2. *Proc Natl Acad Sci U S A* **116**, 15463-15468 (2019).
66. Adelman, K. & Lis, J.T. Promoter-proximal pausing of RNA polymerase II: emerging roles in metazoans. *Nat Rev Genet* **13**, 720-31 (2012).
67. Bunch, H. & Calderwood, S.K. TRIM28 as a novel transcriptional elongation factor. *BMC Mol Biol* **16**, 14 (2015).
68. Haffner, M.C. et al. Androgen-induced TOP2B-mediated double-strand breaks and prostate cancer gene rearrangements. *Nat Genet* **42**, 668-75 (2010).
69. Ju, B.G. et al. A topoisomerase IIbeta-mediated dsDNA break required for regulated transcription. *Science* **312**, 1798-802 (2006).
70. Schmidt, C.K. et al. Systematic E2 screening reveals a UBE2D-RNF138-CtIP axis promoting DNA repair. *Nat Cell Biol* **17**, 1458-1470 (2015).
71. Lee, J.Y. et al. Accumulation of p53 via down-regulation of UBE2D family genes is a critical pathway for cadmium-induced renal toxicity. *Sci Rep* **6**, 21968 (2016).
72. Critchley, W.R., Smith, G.A., Zachary, I.C., Harrison, M.A. & Ponnambalam, S. The E2 ubiquitin-conjugating enzymes UBE2D1 and UBE2D2 regulate VEGFR2 dynamics and endothelial function. *J Cell Sci* **136**(2023).
73. Wu, X. & Karin, M. Emerging roles of Lys63-linked polyubiquitylation in immune responses. *Immunol Rev* **266**, 161-74 (2015).
74. Hofmann, R.M. & Pickart, C.M. Noncanonical MMS2-encoded ubiquitin-conjugating enzyme functions in assembly of novel polyubiquitin chains for DNA repair. *Cell* **96**, 645-53 (1999).
75. Malamos, P. et al. The Interplay between the DNA Damage Response (DDR) Network and the Mitogen-Activated Protein Kinase (MAPK) Signaling Pathway in Multiple Myeloma. *Int J Mol Sci* **25**(2024).
76. Yang, C., Tian, C., Hoffman, T.E., Jacobsen, N.K. & Spencer, S.L. Melanoma subpopulations that rapidly escape MAPK pathway inhibition incur DNA damage and rely on stress signalling. *Nat Commun* **12**, 1747 (2021).
77. Yang, Y. et al. HIF-1 Interacts with TRIM28 and DNA-PK to release paused RNA polymerase II and activate target gene transcription in response to hypoxia. *Nat Commun* **13**, 316 (2022).
78. Haffner, M.C., De Marzo, A.M., Meeker, A.K., Nelson, W.G. & Yegnasubramanian, S. Transcription-induced DNA double strand breaks: both oncogenic force and potential therapeutic target? *Clin Cancer Res* **17**, 3858-64 (2011).
79. van de Kooij, B., Kruswick, A., van Attikum, H. & Yaffe, M.B. Multi-pathway DNA-repair reporters reveal competition between end-joining, single-strand annealing and homologous recombination at Cas9-induced DNA double-strand breaks. *Nat Commun* **13**, 5295 (2022).
80. Davis, A.J. et al. BRCA1 modulates the autophosphorylation status of DNA-PKcs in S phase of the cell cycle. *Nucleic Acids Res* **42**, 11487-501 (2014).

Acknowledgments

We are grateful to D. Engelberg and N. Soudah at the Hebrew University of Jerusalem for their generosity in sharing the bacterial WT and mutant human ERK1/2 expression vectors, to J. Chang's laboratory at Kyungpook National University (KNU) for purifying the ERK proteins, to Rokit Genomics for performing RNA-sequencing analysis, to Enago for proofreading the manuscript, and to Ubigene

Biosciences for generating and validating the BARD1 heterozygous KO HEK293 cells for this work. We thank H. Cho at Ajou University Medical School for sharing critical resources and materials. We also thank D. Kim, C. Jung, S. Ju, and the current members of the Bunch laboratory members at KNU for their technical assistance. H.B. thanks R. S. Baker, John and D. Bunch, and J. Christ for their loving encouragement and support throughout the course of this work. This research was supported by grants from the National Research Foundation (NRF) of the Republic of Korea (2022R1A21003569, RS-2025-02303149, and RS-2025-16067324) to H.B.

Author Contributions

HB performed cell culture, drug treatment, siRNA-mediated factor KD, ChIP-qPCR, total RNA preparation for sequencing, ICE assay, and immunoblotting. HB and JhJ performed qRT-PCR, *in vitro* kinase and ubiquitination assays and prepared for mass spectrometry samples. RN carried out and analyzed mass spectrometry. AC and MS purified and prepared for BARD1, BRCA1-BARD1, and TOP2B proteins. JyJ, IJ, KK performed bioinformatics analysis of RNA-seq data. HB created the hypothesis, designed and coordinated the experiments, analyzed and curated the data, and wrote and revised the manuscript.

Competing Interests Statement

The authors declare that they have no competing interests.

Figure Legends

Fig. 1. BRCA1-BARD1 assembles with E2 enzymes, UBCH5b or UBC13/MMS2, to ubiquitinate TOP2B

(**A**) Statistical summary of the *in vitro* ubiquitination assay and immunoblotting-based quantification results. A total of commercially available, 11 human E2 enzymes were screened, among which UBCH5b and UCB13/MMS2 were identified to interact with BRCA1-BARD1 (E3 ligase) and UBE1 (E1) to ubiquitinate TOP2B (substrate).

(**B**) Left, Coomassie-blue stained control TOP2B and BRCA1-BARD1 proteins used for the *in vitro* ubiquitination and mass spectrometry analyses. Ubiquitinated residues identified in the control samples were listed under the gel image. SM, standard protein size marker. Right, post-*in vitro* ubiquitinated TOP2B samples on a SDS-PAGE gel, which were sliced and analyzed by mass spectrometry.

(**C**) The residues identified to be ubiquitinated by UBCH5b-BRCA1-BARD1 (light blue diamonds, n = 35) or UBC13/MMS2-BRCA1-BARD1 (red circles, n = 5) were marked on TOP2B protein, showing distinctive patterns and specificities of TOP2B ubiquitination by BRCA1-BARD1, depending on partnering E2 enzymes. Note that the resides ubiquitinated by UBC13/MMS2-BRCA1-BARD1 were mapped only in the DNA binding and catalysis domain. Four sites, K643, K744, K979, and K1079 were mutually identified between two groups, with UBC13/MMS2-unique site, K510.

(**D**) The residues identified to be ubiquitinated by UBCH5b-BRCA1-BARD1 (light blue diamonds) or UBC13/MMS2-BRCA1-BARD1 were marked on BARD1 and BRCA1 proteins (red circles).

Fig. 2. BARD1, UBCH5b, or UBC13 knockdown deregulates TOP2B and represses IEG transcription

(**A**) Immunoblotting results. Left, BARD1 KD validation. Middle, UBCH5b KD validation. Right, UBC13 KD validation. SCR, scrambled, non-specific siRNA control. ACTIN was used as a reference gene and a loading control.

(**B**) Summary of multiple immunoblotting results and statistical validations (n = 3 independent experiments). Data are presented as mean values and standard deviations (SDs). *P*-values for the bar graphs were calculated with the unpaired, one sided Student's t-test. $^{**}P < 0.01$, $^{***}P < 0.005$.

(**C**) ChIP-qPCR results showing TOP2B occupancy changes in the TSSs of representative IEGs, *EGR1*, *FOS*, *JUN*, and *MYC*, comparing mock-treated (Mock), UBCH5b KD, or UBC13 KD HEK293 cells (n = 3 independent experiments). Data are presented as mean values and SD. *P*-values for the bar graphs were calculated with the unpaired, one sided Student's t-test. $^{**}P < 0.01$, $^{***}P < 0.005$, $^{****}P < 0.0005$.

(**D**) ChIP-qPCR results showing TOP2A occupancy changes in the TSSs of representative IEGs, *EGR1*, *FOS*, *JUN*, and *MYC*, comparing mock-treated (Mock), UBCH5b KD, or UBC13 KD HEK293 cells (n = 3 independent experiments). Data are presented as mean values and SD. *P*-values for the bar graphs were calculated with the unpaired, one sided Student's t-test. $^{*}P < 0.05$, $^{**}P < 0.01$, $^{***}P < 0.005$, $^{****}P < 0.0005$.

(**E**) Representative ICE assay results showing the effects of UBCH5b or UBC13/MMS2 KD in comparison with the control (Mock). When indicated (+ Eto), etoposide was supplemented to a final concentration of 50 μM for 1 h. The control samples (- Eto) were treated with the same amount of DMSO. Chromosome-bound TOP2B was quantified using immunoblotting.

(**F**) qRT-PCR results showing the repressive effects of BARD1, UBCH5b or UBC13 KD at the *EGR1*, *FOS*, *JUN*, and *MYC* genes, compared to the SCR control in HEK293 cells (n = 3 biologically independent samples). Data are presented as mean values and SD. *P*-values for the bar graphs were calculated with the unpaired, one sided Student's t-test. $^{*}P < 0.05$, $^{**}P < 0.01$, $^{***}P < 0.005$, $^{****}P < 0.0005$.

(**G**) qRT-PCR results indicating transcriptional repression in both S0 and S15 conditions at the *EGR1*, *FOS*, and *JUN* genes in HEK293 cells lacking BARD1, UBCH5b, or UBC13 (n = 3 biologically independent samples). Data are presented as mean values and SD. *P*-values for the bar graphs were calculated with the unpaired, one sided Student's t-test. $^{**}P < 0.01$, $^{***}P < 0.005$, $^{****}P < 0.0005$.

Fig. 3. A transcription-regulatory circuit between BARD1 and mitogen-activated protein kinase pathway

(**A**) Immunoblotting results showing protein expression levels of BARD1, TOP2B, TOP2A, and γH2AX in WT and BARD1 KD^{hz} HEK293 cells. ACTIN, a reference gene and a loading control.

(**B**) Immunoblotting data showing UBCH5b and UBC13 protein levels in WT and BARD1 KD^{hz} HEK293 cells. ACTIN, a reference gene and a loading control.

(**C**) A volcano plot showing DEGs (|Log_2FC| > 1 and adjusted *P*-value < 0.05) from RNA-seq data (n = 3), comparing WT and BARD1 KD^{hz} HEK293 cells. NS, non-significant.
(**D**) Relative mRNA expression fold changes of representative IEGs, *EGR1*, *FOS*, *JUN*, and *MYC* in WT and BARD1 KD^{hz} HEK293 cells.
(**E**) Heatmaps of DEGs, comparing WT and BARD1 KD^{hz} HEK293 cells.
(**F**) KEGG pathway analysis with DEGs, comparing WT and BARD1 KD^{hz} HEK293 cells.
(**G**) mRNA expression of key factors, *RAF1*, *NRAS*, *HRAS*, *JNK1*, and *JNK2* in MAPK pathway in WT and BARD1 KD^{hz} HEK293 cells.
(**H**) mRNA expression of *ERK1* and *ERK2* in WT and BARD1 KD^{hz} HEK293 cells.

Fig. 4. Activated ERK2 phosphorylates BARD1 at S391, a pathologically important residue for IEG activation
(**A**) Autoradiograms of the *in vitro* kinase assay with BARD1 and ERKs.
(**B**) *In vitro* kinase assay followed by SDS-PAGE for the preparation of BARD1 samples for mass spectrometry analyses. Red boxes showing sliced gel pieces including BARD1 used for the analyses. CTRL, ERK storage buffer only without ERKs; SM, size marker (KDa).
(**C**) A flow chart showing the major steps of mass spectrometry analyses performed in this work.
(**D**) Summary of the phosphorylated residues of BARD1 in the control, ERK1m, and ERK2m reactions identified by mass spectrometry analyses and their scores. The residues with high confidence and statistical significance are marked with colors.
(**E**) A schematic representation of the BARD1 residues phosphorylated by ERK2m (a red and purple circles) and ERK1m (green triangles) and in the control (a skyblue and gray squares). The residues identified with high confidence were marked with a skyblue square (S394 in the control BARD1) and a red circle (S391 in BARD1 phosphorylated by ERK2m).
(**F**) ChIP-qPCR results showing BARD1 occupancy changes in the TSSs of representative IEGs, *EGR1* and *FOS*, comparing DMSO- or VX11-treated cells in S0 and S15 conditions (n = 3 independent experiments). Data are presented as mean values and SD. *P*-values for the bar graphs were calculated with the unpaired, one sided Student's t-test. **P* < 0.05, ****P* < 0.005, *****P* < 0.0005.
(**G**) ChIP-qPCR results showing S2 Pol II occupancy changes in the TSSs of representative IEGs, *EGR1* and *FOS*, comparing DMSO- or VX11-treated cells in S0 and S15 conditions (n = 3

independent experiments). Data are presented as mean values and SD. *P*-values for the bar graphs were calculated with the unpaired, one sided Student's t-test. ****$P < 0.0005$.

(**H**) ChIP-qPCR results showing BARD1 occupancy changes in the TSSs of representative IEGs, *EGR1* and *FOS*, comparing SCR control and ERK2 KD HEK293 cells in S0 and S15 conditions (n = 3 independent experiments). Data are presented as mean values and SD. *P*-values for the bar graphs were calculated with the unpaired, one sided Student's t-test. **$P < 0.01$, ***$P < 0.005$.

(**I**) ChIP-qPCR results showing TOP2B occupancy changes in the TSSs of *EGR1* gene, comparing DMSO- or VX11-treated cells (left) and SCR and ERK2 KD cells (right)(n = 3 independent experiments). Data are presented as mean values and SD. *P*-values for the bar graphs were calculated with the unpaired, one sided Student's t-test. **$P < 0.01$, ****$P < 0.0005$.

Fig. 5. BARD1 phosphorylation by activated ERK2 enhances UBCH5b- and UBC13/MMS2-mediated TOP2B ubiquitination

(**A**) Silver-stained SDS PAGE gels showing BRCA1-BARD1 purified as a complex from HEK293 cells (left), ERK2m purified from *E. coli* (middle), and TOP2B from HEK293 cells (right). IN, input protein mixtures including BRCA1-BARD1 loaded onto a sizing exclusion column.

(**B**) Immunoblotting results verifying TOP2B (upper left), ERK2m (bottom left), and BRCA1-BARD1 (right).

(**C**) Silver-stained SDS-PAGE gel showing a portion (22%) of the reactions immediately after the *in vitro* ubiquitination assay.

(**D**) Immunoblotting results showing TOP2B ubiquitinated by UBCH5b-BRCA1-BARD1 (red boxes) or UBC13/MMS-BRCA1-BARD1 (skyblue boxes) in the absence and presence of ERK2m. A band, corresponding presumably to a higher molecular-weighted, poly-ubiquitinated TOP2B, with UBCH5b-BRCA1-BARD1 becomes more intense in the presence of ERK2m (marked with a red asterisk). VX11 supplement along with ERK2m interferes with stimulated ERK2m-mediated TOP2B ubiquitination by UBCH5b-BRCA1-BARD1 and UBC13/MMS-BRCA1-BARD1 (green boxes). Ubiquitin (Ubi) and TOP2B blots were developed for a longer (long exp) and shorter (short exp) period for better presenting the bands.

Fig. 6. A proposed model: the triangular relationship of TOP2B, BARD1, and ERK2 for human IEG transcription.

Based on the findings, we propose a gene regulatory model involving dynamic interactions among a critical DNA topology regulator, a DNA repair factor, and a transcriptional activator, TOP2B, BRCA1-BARD1, and ERK2m in IEG transcription. In Pol II pausing during the transcriptionally resting state, BRCA1-BARD1 ubiquitinates TOP2B, which increases TOP2B stability and affinity with the IEG TSSs[1,29]. Upon the reception of a signal to progress the cell cycle to the G1 phase, ERK2 is phosphorylated and activated in the cytoplasm and translocates into the nucleus[40]. Activated ERK2 phosphorylates BARD1 at S391 (**Figs. 4A–E**) and other previously reported substrates, TOP2B, and ELK1[14]. BARD1/TOP2B phosphorylation by ERK2 and TOP2B ubiquitination by ERK2-stimulated UBCH5b-BRCA1-BARD1 and UBC13-BRCA1-BARD1 are important for proper BARD1/TOP2B engagement and productive IEG transcription (**Figs. 2C,E–G,3C,D,4A–I,5D**). Our data suggest that TOP2B ubiquitination by UBCH5b-BRCA1-BARD1 may promote TOP2B-gene interaction and TOP2B degradation whereas TOP2B ubiquitination by UBC13/MMS2-BRCA1-BARD1 may enhance TOP2B catalysis and stabilize TOP2B (**Figs. 2A–C,E**). Pol II pause release is coupled with TOP2B catalysis and DDR signaling, which involves the activation of DNA repair factors including ATM, ATR, and DNA-PK[1,30,41].

Figures.

Figure 1.

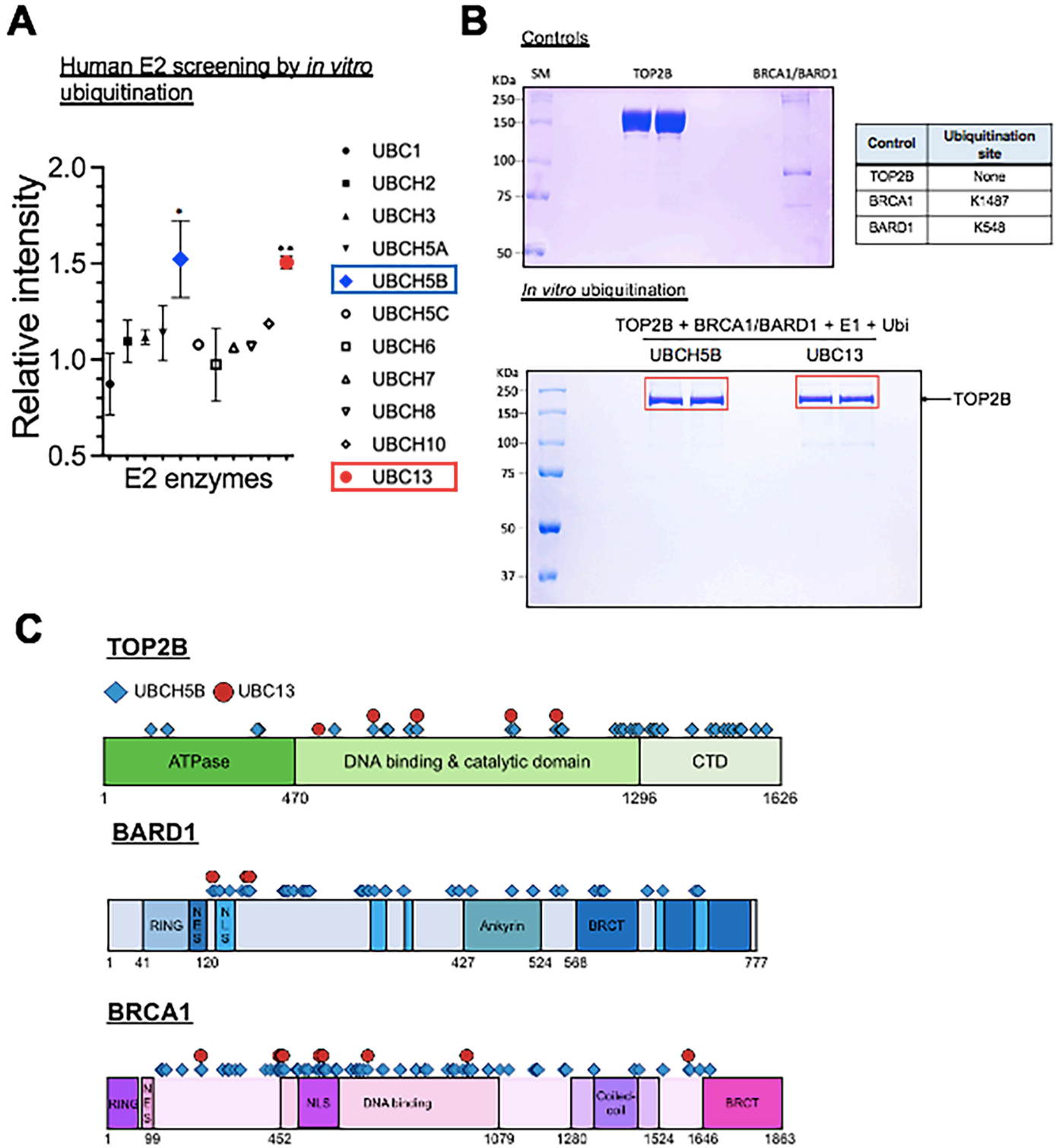

Figure 1-Bunch *et al.*

Figure. 2.

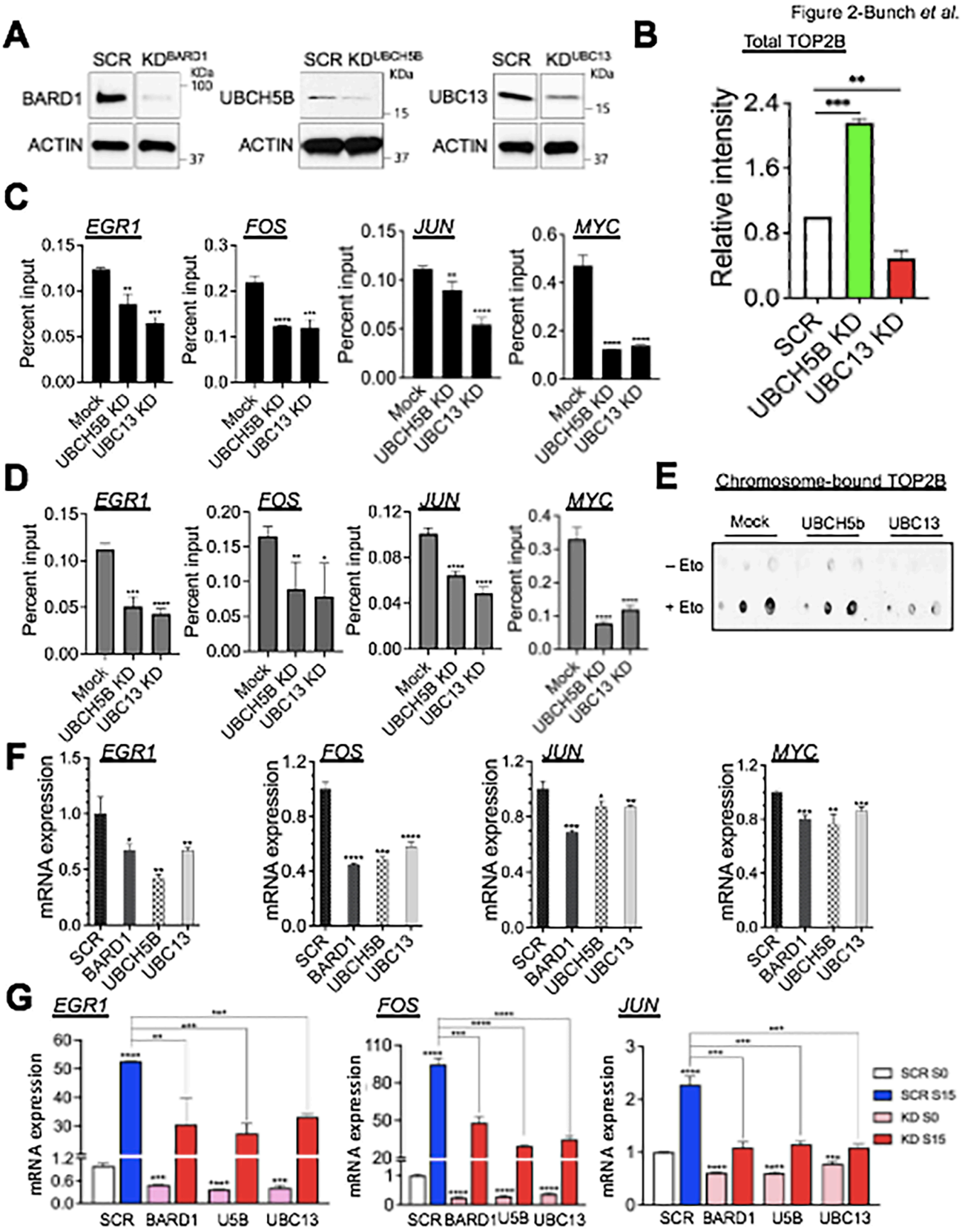
Figure 2-Bunch et al.
A
SCR KD BARD1
KDa
100
BARD1
ACTIN
37
SCR KD UBCH5B
KDa
UBCH5B
15
ACTIN
37
SCR KD UBC13
KDa
UBC13
15
ACTIN
37
B
Total TOP2B
Relative intensity
2.4
1.6
0.8
0.0
SCR
UBCH5B KD
UBC13 KD
C
EGR1
FOS
JUN
MYC
Percent input
Mock
UBCH5B KD
UBC13 KD
D
EGR1
FOS
JUN
MYC
Percent input
Mock
UBCH5B KD
UBC13 KD
E
Chromosome-bound TOP2B
Mock
UBCH5b
UBC13
– Eto
+ Eto
F
EGR1
FOS
JUN
MYC
mRNA expression
SCR
BARD1
UBCH5B
UBC13
G
EGR1
FOS
JUN
mRNA expression
SCR
BARD1
U5B
UBC13
SCR S0
SCR S15
KD S0
KD S15

Figure 3.

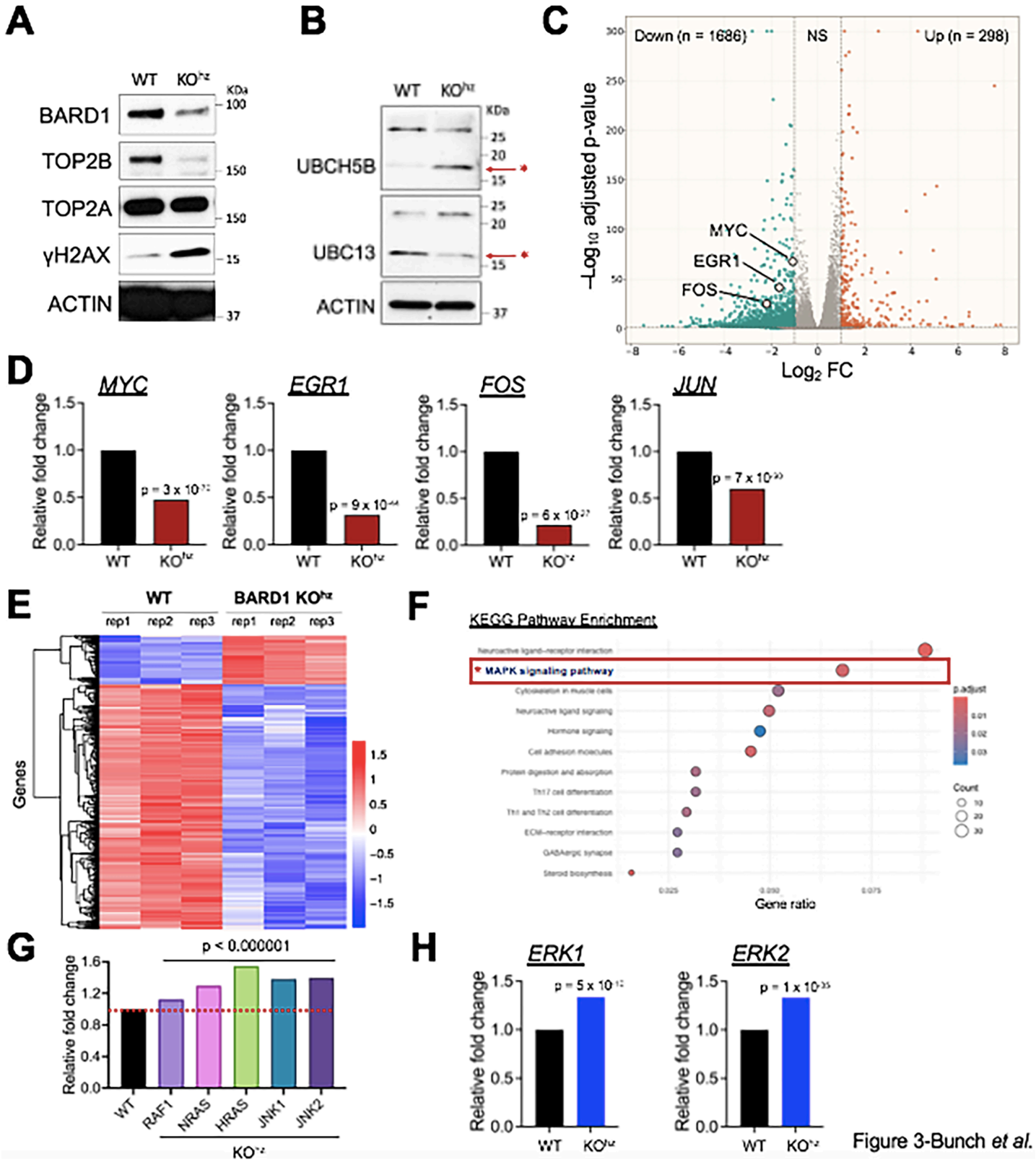

Figure 3-Bunch *et al.*

Figure 4.

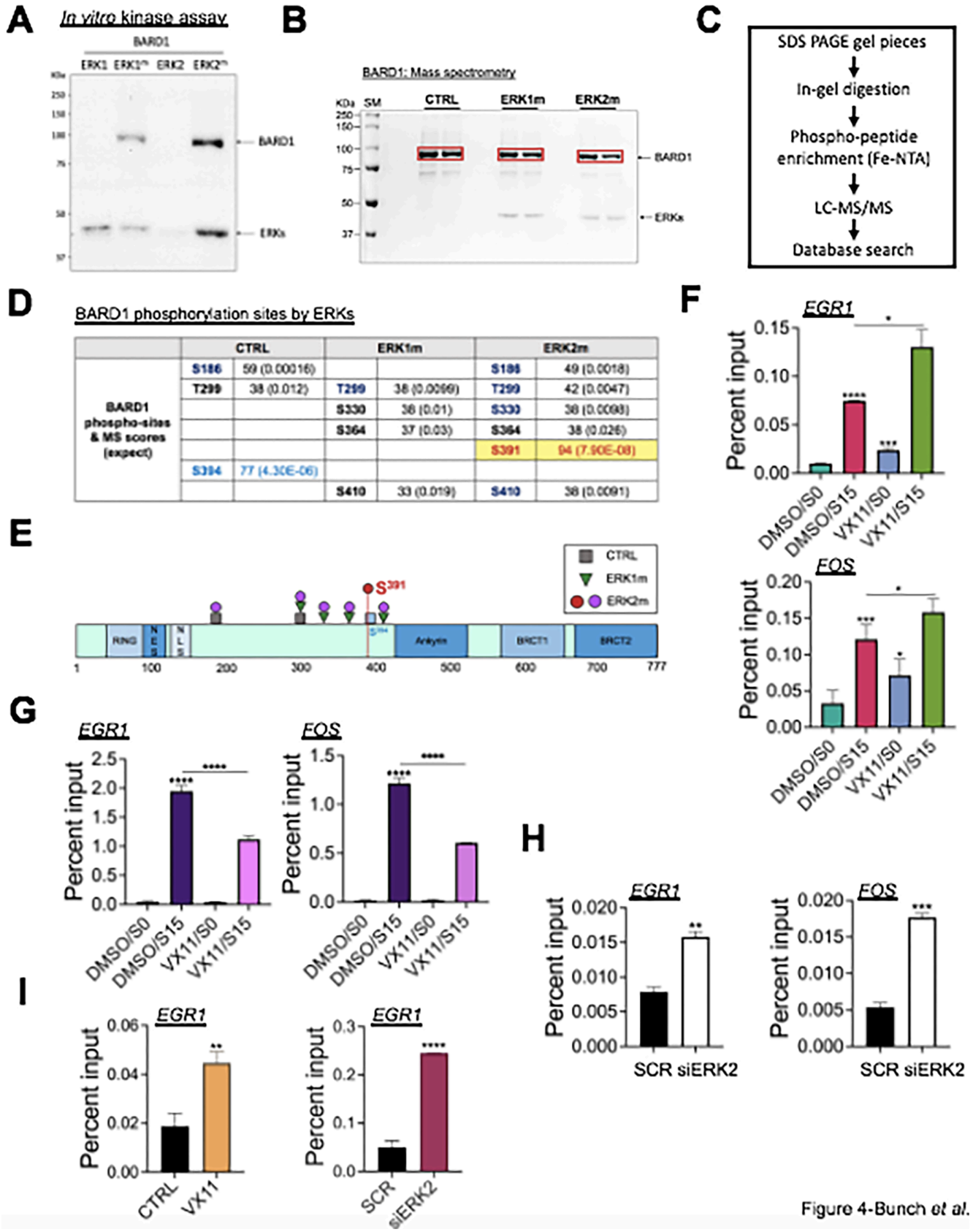

Figure 4-Bunch *et al.*

Figure 5.

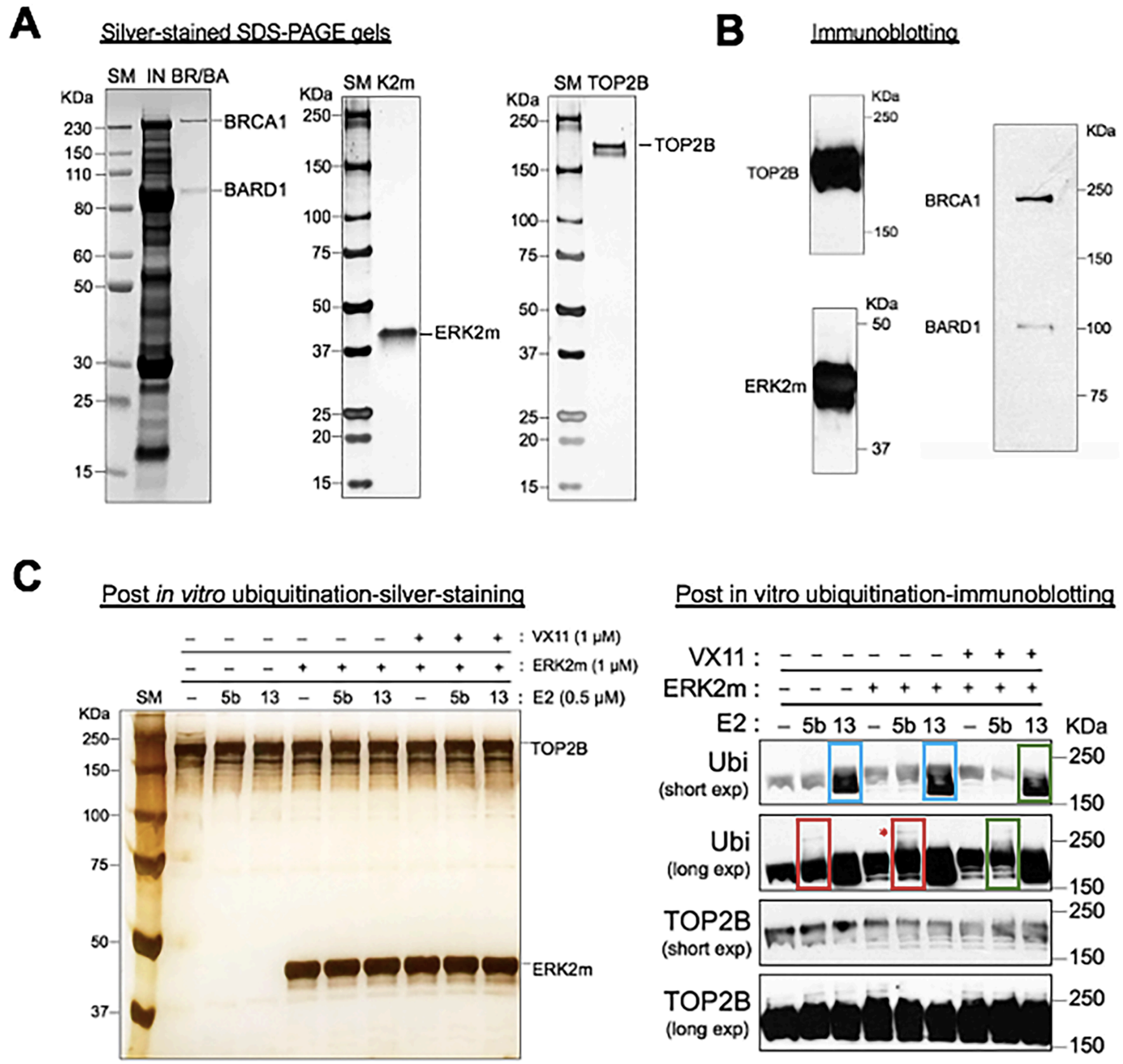

Figure 5-Bunch *et al.*

Figure 6.

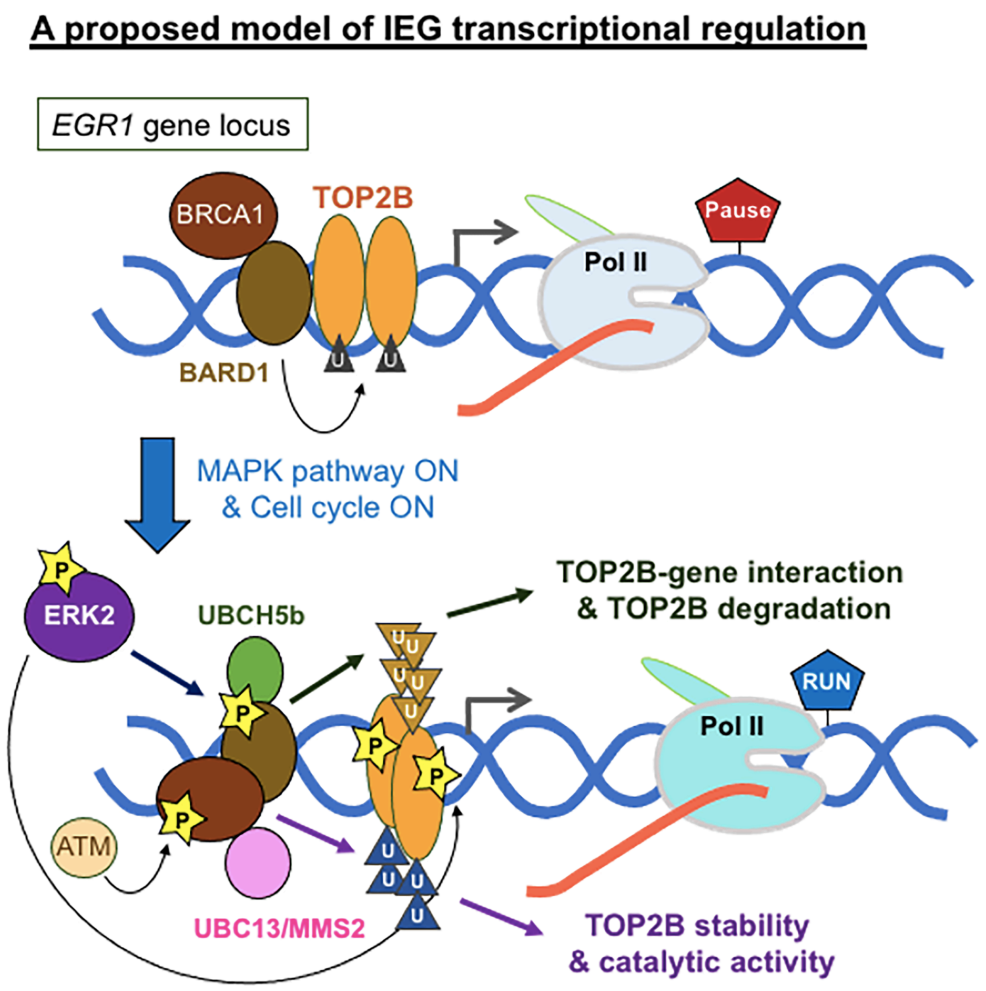

Figure 6-Bunch *et al.*